Applied Catalysis B: Environmental 90 (2009) 249–254

Contents lists available at ScienceDirect

Applied Catalysis B: Environmental

journal homepage: www.elsevier.com/locate/apcatb

Visible light photocatalytic activity of TiO_2/D-PVA for MO degradation

Yongzhong Wang, Mingqiang Zhong *, Feng Chen, Jintao Yang

College of Chemical Engineering and Materials Science, Zhejiang University of Technology, Hangzhou 310014, China

ARTICLE INFO

Article history:
Received 3 December 2008
Received in revised form 2 March 2009
Accepted 5 March 2009
Available online 5 April 2009

Keywords:
TiO_2/D-PVA
Visible light photocatalysis
Hydrothermal method
Methyl orange
Degradation kinetics

ABSTRACT

A novel visible light (VL) active photocatalyst (TiO_2/D-PVA) was prepared in one portion of polyvinyl alcohol (PVA) and $Ti(OH)_4$ by means of hydrothermal method, and the relationship between the prepared conditions and VL photocatalytic activity was investigated. The synthesized photocatalyst was characterized by XRD, UV–vis, XPS, FTIR and EPR. The results show that PVA was dehydrated to produce conjugated unsaturated D-PVA. The VL photocatalytic activity was attributed to the interaction between D-PVA and TiO_2. The TiO_2/D-PVA, synthesized with the 1:10 feed ratio of PVA to TiO_2 at 180 °C, exhibited a significant VL activity for the Methyl orange (MO) degradation. The degradation rate fit the characteristic of apparent first-order kinetics. The mechanism of MO degradation was also proposed.

1. Introduction

TiO_2 is well known as a matter with strong redox ability, and used for water or air purification [1,2] and photoelectrochemical cell [3,4], due to its cheapness, nontoxicity and high photocatalytic activity. However, it can only absorb UV (ultraviolet light, <387 nm, which constitutes 4% of the solar light) owing to its wide energy gap (3.2 eV). A few methods have been developed to shift its optical response to the visible light (VL) region. Doping transition metals on TiO_2 were investigated [5–8], the improvement of VL absorption about these metal-doped photocatalysts, however, was not significant. Furthermore, producing reduced TiO_x photocatalysts [9–11] or doping nonmetals (N [12–14], C [15–19] and S [20]) on TiO_2 were studied in detail: although the energy gap of TiO_2 could be efficiently narrowed and shifted its optical response to VL region, the preparations needed complicated processes. Recently, some dyes [21–23] and conjugated unsaturated polymers [24–28] were employed as photosensitizer on TiO_2 to produce the optical response of VL. For example, Su et al. [24] prepared TiO_2/polymer by calcinating mixture of $Ti(OH)_4$ and polymer, and the optical response was shifted to VL region apparently. Song et al. [25] prepared the VL active TiO_2/PFT photocatalyst, and proposed the photosensitized degradation mechanism. The conjugated unsaturated polymer is similar in photosensitized mechanism to the dye on TiO_2 under VL. The sensitizer molecules adsorbed on TiO_2 are excited by VL and electrons are subsequently injected to conduction band (CB) of TiO_2. While the CB acts as a mediator for transferring electrons from the sensitizer to substrate electron acceptors on TiO_2 surface, the valence band (VB) remains unaffected in a typical photosensitization. The excited electrons in CB of TiO_2 create a series of chain reactions. The general photosensitized degradation mechanism was shown in Scheme 1.

In our research, a novel VL active photocatalyst (TiO_2/D-PVA) was successfully prepared in one portion of polyvinyl alcohol (PVA) and $Ti(OH)_4$ by means of hydrothermal method. To the best of our knowledge, hydrothermal method was firstly reported to produce TiO_2/polymer composite. The synthesized composite could effectively degrade Methyl orange (MO) under VL irradiation. Due to its low cost and convenient process, TiO_2/D-PVA may contribute to application to the disposal of industrial pollutants.

2. Experimental

2.1. Materials and preparation of photocatalyst

Titanyl sulfate ($TiOSO_4{\cdot}2H_2O$ mass content of 46%, Liaoning Dandong Zhonghe Chemical factory, China), NaOH (Analytical reagent), $Ba(NO_3)_2$ (Analytical reagent), PVA (polymerization degree of 124, Sinopharma, China), MO (Shanghai San'aisi Reagent Co. Ltd., China) and P25 (20% rutile and 80% anatase, Degussa, Germany) were used as received.

106.5 g titanyl sulfate was mixed with 300 mL deionized water in a 1000 mL flask under continuously stirring for 15 min at 90 °C, then 3.0 mol/L NaOH aqueous solution was added dropwise until the pH value reached 8.0. The white mixture was stirred for

* Corresponding author.
E-mail address: zhongmq@zjut.edu.cn (M. Zhong).

0926-3373/$ – see front matter © 2009 Published by Elsevier B.V.
doi:10.1016/j.apcatb.2009.03.032

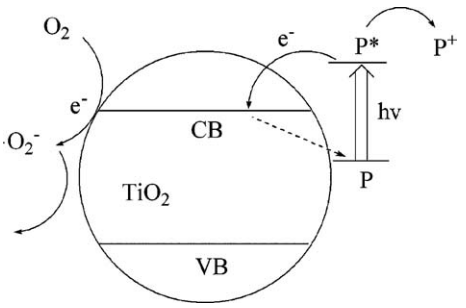

Scheme 1. Photosensitized degradation mechanism of TiO_2/polymer. P stands for sensitizer; P^*, photoexcited sensitizer; P^+, oxidized sensitizer.

another 2 h, and the amorphous $Ti(OH)_4$ precipitate was collected by filtration and washed with deionized water until no SO_4^{2-} was detected by 0.5 mol/L $Ba(NO_3)_2$ solution.

The TiO_2/D-PVA microscale particles were prepared in one portion by hydrothermal method as following. The synthesized amorphous $Ti(OH)_4$ and a certain mass of PVA were added into 1000 mL deionized water in a 2000 mL stainless autoclave. The autoclave was heated up to certain temperature with a rate of 2.5 °C/min and maintained for certain time under a stirring rate of 300 rpm, then cooled to ambient temperature. After hydrothermal reaction, the precipitate was collected by filtration, gently washed with deionized water several times and dried in an oven at 60 °C for 6 h. The product was grinded in a mortar box. Pure TiO_2 was synthesized by the same process in the absence of PVA. Pure PVA was also processed by the same process in the absence of $Ti(OH)_4$.

2.2. Characterization

The surface area of the powders was measured by nitrogen adsorption using the BET equation at 77K (Micrometrics ASAO 2020M+C, America).

The mass of degraded PVA (D-PVA) of photocatalyst was measured under the oxygen atmosphere by TGA (DSC1+TGA/DSC1, METTLER TOLEDO, Switzerland).

The powder X-ray diffraction (XRD) pattern was collected on a Thermo ARL SCLNTAG X'TRA X-ray diffractometer using Cu Kα radiation (λ = 1.54178 Å) operated at 40 kV and 40 mA at a scan rate of 4.0°/min. The average crystallite size was calculated from Scherrer equation ($d = 0.9\lambda/\beta_{1/2}\cos\theta$, where λ is the characteristic X-ray wavelength applied, $\beta_{1/2}$ is the half width of the peak at the 2θ value).

A UV–vis spectrophotometer (UV-2550, Shimadzu, Japan) was used to obtain the UV–vis reflectance spectrum of the powder sample.

The X-ray photoelectron spectroscopy (XPS) was recorded with a Thermo ESCALAB 250 spectrometer using a radiation source of monochromatic Al Kα with the energy of 1486.6 eV, 200 W.

The X-band electron paramagnetic resonance (EPR) spectrum was recorded at 293 K using a Bruker A300 EPR spectrometer with 9867 MHz.

The IR spectrum was characterized with a Nicolet 6700 FTIR spectrometer, using KBr pellet for sample preparation.

2.3. VL photocatalytic degradation

The photocatalytic activities of the samples were evaluated by the degradation of MO in an aqueous solution. 200 mL MO solution (10 mg/L) and 0.5 g photocatalyst was put into a 1 L beaker which was surrounded by circulated water to cool at 25 °C. A 200 W dysprosium lamp (Institute of Electrical Light Source, Beijing, China), used as the VL irradiation source, was positioned over MO solution at the height of 16 cm. A 400 nm filter was used to cut off UV light below 400 nm. Before irradiation, the solution was continuously stirred for 45 min to ensure the establishment of an adsorption–desorption equilibrium between the photocatalyst and MO. After the suspension was irradiated for certain time, 4 mL suspension was taken out and centrifugalized, then the MO concentration of clean solution was measured by a 722 spectrometer (Shanghai third analysis instrument factory, China).

The photocatalytic activity lifetime of TiO_2/D-PVA was carried out as following. After the mixture of 200 mL MO solution (10 mg/L) and 0.5 g TiO_2/D-PVA sample was irradiated for 40 h with the same conditions above, the TiO_2/D-PVA sample was carefully collected by centrifugalization and then was dried in an oven at 60 °C for 6 h. The next cycle test was done using the collected TiO_2/D-PVA and 200 mL MO solution (10 mg/L). In our test, the loss of TiO_2/D-PVA had been measured by gravimetry and was tiny.

3. Results and discussion

$Ti(OH)_4$ was degraded to produce TiO_2, and PVA was degraded to produce conjugated unsaturated D-PVA, which was accelerated by the synthesized TiO_2 as a Lewis acid under hydrothermal process. The synthesized TiO_2/D-PVA was characterized by XRD, UV–vis, XPS, FTIR and EPR. The feed ratio of PVA to TiO_2 and hydrothermal temperature were investigated for VL absorption and MO degradation properties of TiO_2/D-PVA.

3.1. The characterization of TiO_2/D-PVA

The XPS spectrum (Fig. 1a) reveals that the Ti2p core level of TiO_2/D-PVA consists of two peaks with binding energy of 458.5 and 464.4 eV for $Ti^{4+}2p_{3/2}$ and $Ti^{4+}2p_{1/2}$, respectively. This result also exhibits no existence of the lower valence of Ti ion [9]. The C 1s peaks of XPS spectrum (Fig. 1b) occur at 284.9, 286.3 and 288.9 eV. The peak of 284.9 eV is assigned to adventitious elemental carbon remained in D-PVA, and the other two small peaks indicate the existence of C–O and C═O [15,16,18,19]. The O 1s peaks of XPS spectrum (Fig. 1c) occurred at 532.6, 531.3 and 529.7 eV are assigned to C–O, OH on the surface of TiO_2 and Ti–O–Ti, respectively [29]. Because the O 1s signal of C═O is very weak, it is not shown in Fig. 1c. K. Sugiyama et al. [9] synthesized TiO_2 by the CH_4–H_2 plasma CVD method. The TiO_2 treated by plasma heating showed a shoulder peak of 282 eV which was assigned to C 1s of Ti-C. Hashimoto et al. [30] prepared carbon-doped titania by oxidizing TiC, and observed C 1s XPS peak with much lower binding energy (281.8 eV) due to the existence of Ti–C bond. These results were supposed that some carbon atoms substituted for some lattice oxygen atoms of TiO_2. Therefore, in our research, there is no carbon atom of D-PVA integrated with titanium, and D-PVA does not exist in the crystal lattice of TiO_2, which indicates that D-PVA is only doped onto the surface of TiO_2.

Fig. 2 shows the photoinduced EPR data of the pure TiO_2 and TiO_2/D-PVA. TiO_2/D-PVA appears a distinct signal at $g = 2.0166$ which is attributed to the photoexcited π electrons of C═C, and pure TiO_2 gives no response. Gou et al. [28] prepared the TiO_2/conjugated polymer complex whose ESR signal was shown at $g = 2.0035$. van Hal et al. [26] reported that TiO_2/MEH-PPV showed a distinct ESR signal of conjugated C═C bond at $g = 2.0026$. The difference of g-factor may ascribe to the difference of measure condition, or to the other structure in TiO_2/D-PVA, which requires more research. The TiO_2/D-PVA sample shows a strong response signal, which ascribes to the interaction between D-PVA and TiO_2. The electrons which are excited from $\pi \rightarrow \pi^*$ of D-PVA can easily be injected into the CB of TiO_2 [26], so the separation between electrons and cavities becomes easier. Compared to the pure TiO_2,

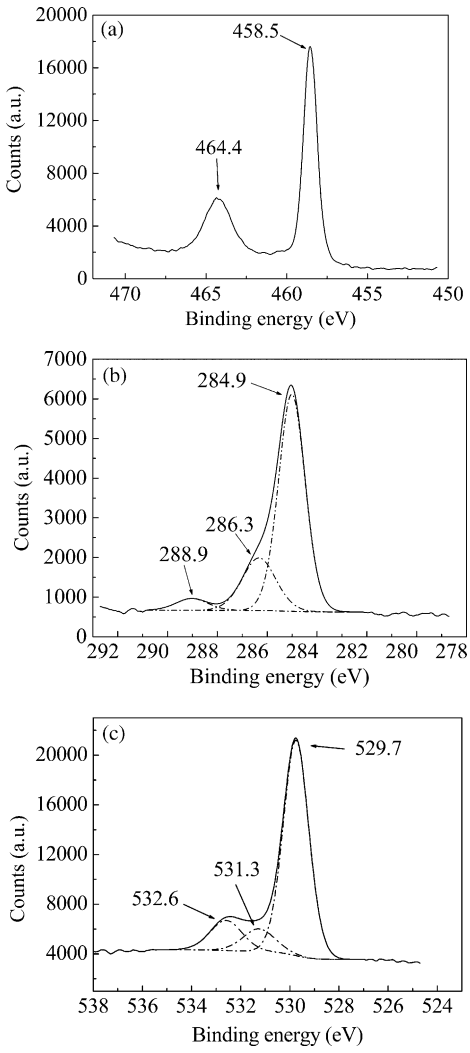

Fig. 1. XPS spectra of Ti2p (a), C 1s (b) and O 1s (c) of TiO_2/D-PVA. The sample was prepared at 180 °C with the reaction time for 6 h and the 1:10 feed ratio of PVA to TiO_2.

the VL response intensity and photocatalytic activity of TiO_2/D-PVA can greatly be improved.

FTIR was used to obtain further information of the structure of TiO_2/D-PVA (As shown in Fig. 3). The peak of near 1640 cm^{-1} is assigned to –OH bond vibration of H_2O absorbed and hydroxy group on the surface of the catalyst, and the new peak of near

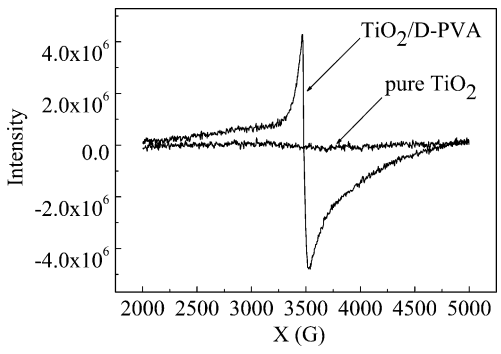

Fig. 2. EPR spectra of TiO_2/D-PVA and pure TiO_2. The TiO_2/D-PVA sample was prepared at 180 °C with the reaction time for 6 h and the 1:10 feed ratio of PVA to TiO_2.

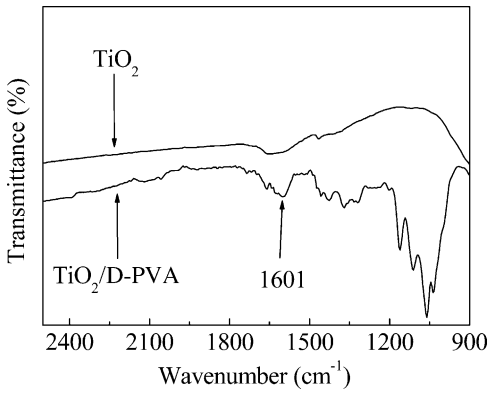

Fig. 3. FTIR spectra of TiO_2 and TiO_2/D-PVA. The TiO_2/D-PVA sample was prepared at 180 °C with the reaction time for 6 h and the 1:10 feed ratio of PVA to TiO_2. The samples had been dried under vacuum at 60 °C for 48 h.

1601 cm^{-1} is assigned to conjugated C=C bond stretching and broadened due to long conjugation chain. The characteristic peaks assigned to C=C=C, C=C=O, C≡C and cyclic conjugated structures do not appear, so it can be inferred that D-PVA is linear unsaturated. In comparison with TiO_2, the FTIR spectrum of TiO_2/D-PVA shows a strong and broad absorption in the region of 950–1200 cm^{-1}, which indicates that TiO_2 strongly interacts with D-PVA.

Fig. 4 shows the UV–vis diffuse reflectance spectra of TiO_2/D-PVA and pure TiO_2. TiO_2/D-PVA can absorb more UV and VL of the whole VL region (400–800 nm) than pure TiO_2, which ascribes to the conjugated C=C bond. Because the C–O and C=O are not chromophores, the conjugated C=C of D-PVA on the surface of TiO_2 is responsible for VL absorption.

3.2. Effect of the feed ratio of PVA to TiO_2

In order to illustrate the relationship between the VL photocatalytic activity and the content of PVA, we prepared the samples with the various feed ratios of PVA to TiO_2 at 200 °C. The XRD patterns (Fig. 5) characterize that TiO_2 in all the synthesized TiO_2/D-PVA samples consist of anatase structure (JCPDS card 21-1272) with high crystallinity. The average crystallite sizes are between 14.4 nm and 15.4 nm (Table 1). The feed ratio has not obviously effect on the crystallite size.

Table 1 summarizes the characterizations of the samples. TiO_2 is a polar matter and has the tendency of agglomeration, which shows the smallest BET surface area of 60.5 m^2/g. The D-PVA, which is a non-polar polymer, doped on TiO_2 can reduce the

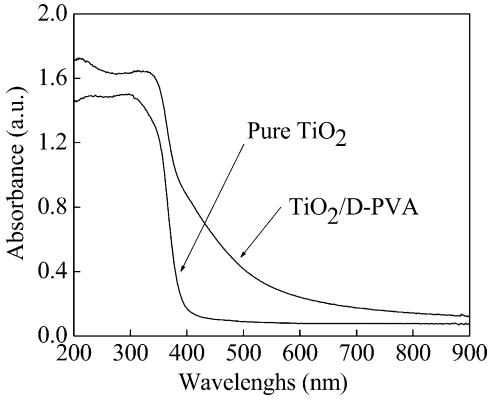

Fig. 4. UV–vis spectra of TiO_2/D-PVA and pure TiO_2. The sample was prepared at 180 °C with the reaction time for 6 h and the 1:10 feed ratio of PVA to TiO_2.

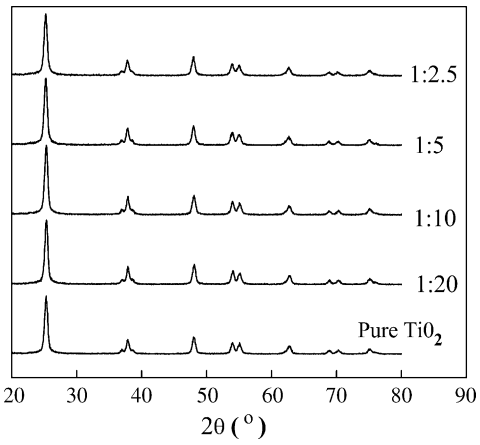

Fig. 5. XRD patterns of pure TiO_2 and TiO_2/D-PVA with the various feed ratios of PVA to TiO_2. All the samples were prepared at 200 °C with the reaction time for 6 h.

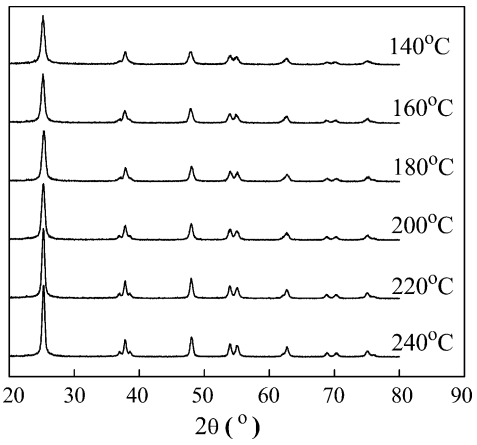

Fig. 6. XRD patterns of TiO_2/D-PVA prepared at different temperature. All the samples were prepared with the 1:10 feed ratio of PVA to TiO_2 and the reaction time for 6 h.

surface tension of TiO_2, so the agglomeration of TiO_2 in TiO_2/D-PVA is greatly decreased. The trend of BET surface area is varied with the feed ratios of PVA to TiO_2: 1:10 > 1:5 > 1:2.5 > 1:20 > pure TiO_2. When the content of D-PVA exceeds 5.8 wt% (1:10 feed ratio of PVA to TiO_2), the surface tension is no longer decreased, and the agglomeration is slightly increased, which exhibits the slightly decrease of BET surface area.

The synthesized TiO_2/D-PVA samples were successfully applied to the MO degradation (Table 1). The TiO_2/D-PVA sample with the 1:10 feed ratio of PVA to TiO_2 shows the higher VL photocatalytic activity under VL irradiation. The effect on MO degradation is related to the active site amount on the surface of TiO_2/D-PVA particles and the D-PVA content. Firstly, the D-PVA, which provides the photoexcited electrons to be injected into the CB of TiO_2, must be doped onto the surface of TiO_2. Secondly, MO molecules must also be absorbed onto the surface of TiO_2 to react with active radicals generated by the photoexcited electrons in the CB of TiO_2. As the feed ratio of PVA to TiO_2 does not exceed 1:10, though D-PVA is almost doped onto TiO_2, the active sites on the surface of TiO_2 are still adequate. However, as the feed ratio of PVA to TiO_2 exceeds 1:10, the excessive D-PVA doped onto TiO_2 occupies the active sites on the surface of TiO_2 and inhibits MO from contacting TiO_2 effectively, so the MO degradation decreases even though the BET surface area does not almost change [31].

3.3. Effect of the hydrothermal temperature

In order to illustrate the relationship between the VL photocatalytic activity and hydrothermal temperature, we prepared the samples with the 1:10 feed ratio of PVA to TiO_2 at the various hydrothermal temperatures. The XRD patterns (Fig. 6) show that the TiO_2 prepared herein is anatase structure. With the elevated hydrothermal temperature, XRD peaks become sharp, and the crystallite sizes become large (Table 2), which indicates that the more uniform crystallite is formed.

Table 2 summarizes the BET surface areas of the TiO_2/D-PVA samples and MO degradation under VL irradiation. The TiO_2/D-PVA sample prepared at 140 °C shows lower catalytic activity due to the inadequate crystallinity of TiO_2 and degradation of PVA in spite of its large BET surface area. The higher VL photocatalytic activity of TiO_2/D-PVA sample prepared at 180 °C is attributed to its large BET surface area and enough D-PVA. However, the TiO_2/D-PVA samples prepared at higher temperatures (≥200 °C) show low catalytic activity because of the following reasons: firstly, PVA is excessively degraded to form layer of carbon (the sample shows obviously fuscous), so the amount of conjugated D-PVA is degraded; Secondly, the formed carbon layer can cover the surface of TiO_2 and inhibit the MO molecules to contact with TiO_2; Thirdly, the high temperature results in a large crystallite size and a low BET surface area [31].

3.4. MO degradation and kinetics research

Fig. 7 shows the MO degradation results photocatalyzed by TiO_2/D-PVA, pure TiO_2 and P25 under VL irradiation. It is obvious that TiO_2/D-PVA shows more effective VL photocatalytic activity. When the suspension system was irradiated for 40 h, the degradation percentage of MO reached 84.0% by TiO_2/D-PVA, compared to 6.5% and 9.2% by pure TiO_2 and P25, respectively. TiO_2 and P25 could degrade a little MO because of the MO self-sensitization. Furthermore, the MO degradation percent still remained 81.6% under 40 h VL irradiation after TiO_2/D-PVA had been used for three cycles viz 120 h.

Table 1
Characteristics of samples prepared with various feed ratios of PVA to TiO_2. All the samples were prepared at 200 °C with the reaction time for 6 h.

Feed ratio of PVA to TiO_2	Crystallite size[a] (nm)	BET surface area[b] (m^2/g)	Mass content of D-PVA[c] (%)	MO degradation (%)
Pure TiO_2	15.4	60.5	0	2.0
1:20	14.9	75.5	3.0	11.2
1:10	14.7	82.2	5.8	28.6
1:5	14.9	81.9	7.6	20.3
1:2.5	14.4	81.1	9.5	17.1

[a] Calculated from Scherrer equation.
[b] Calculated from BET equation.
[c] Calculated from TGA.

Table 2
Characteristics of TiO_2/D-PVA samples prepared at various hydrothermal temperature. All the samples were prepared with the 1:10 feed ratio of PVA to TiO_2 and the reaction time for 6 h.

Temperature (°C)	Crystallite size[a] (nm)	BET surface area[b] (m^2/g)	MO degradation (%)
140	13.4	98.4	24.5
160	14.3	92.3	27.3
180	14.5	86.7	28.3
200	14.9	82.2	20.3
220	17.8	75.8	16.5
240	17.9	65.7	8.8

[a] Calculated from Scherrer equation.
[b] Calculated from BET equation.

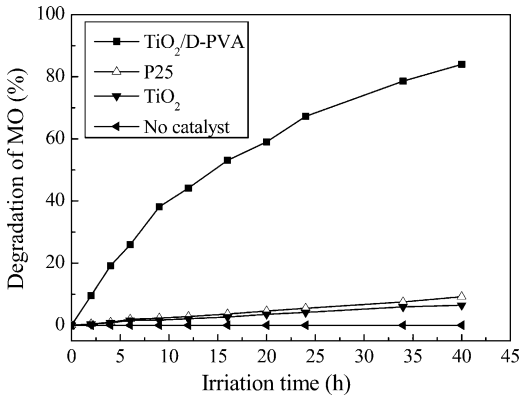

Fig. 7. Curves of MO degradation under VL irradiation. TiO_2/D-PVA was produced at 180 °C with the reaction time for 6 h and the 1:10 feed ratio of PVA to TiO_2.

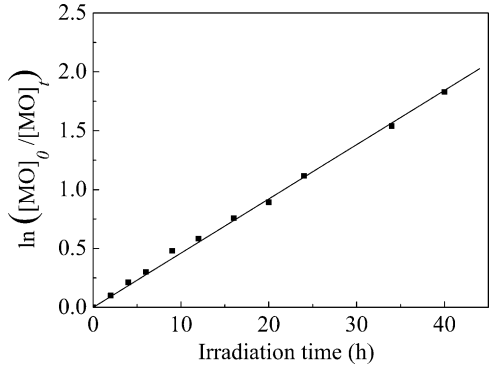

Fig. 8. Relation between the concentration of MO and irradiation time under VL irradiation.

The rate of MO degradation is gradually decreased with the increase of irradiation time (Fig. 8), which fits the characteristic of apparent first-order kinetics and the reaction constant of rate is about 0.0461 h^{-1}.

$$\ln\left(\frac{[MO]_0}{[MO]_t}\right) = 0.0461\,t$$

$[MO]_0$: the concentration of MO before irradiation; $[MO]_t$: the concentration of MO after irradiation for t h.

Song et al. [25] reported that oxygen was very important for an effective photodegradation process. On the one hand, its timely capture of the CB electron effectively restrains the recombination of the CB electron and positive ion of photosensitizer. On the other hand, it participates as a reactant to create a series of active oxides to induce a chain reaction. According to our results and previous studies [25,32,33] on the photocatalytic degradation of organics using polymer-modified TiO_2 under VL irradiation, the mechanism of MO degradation can be represented in Scheme 2.

Due to the short lifetime and high activity of e_{cb}^- and free radical in solution, the reactions of (3)–(11) are taken place only on the surface of photocatalyst, which indicates that MO must be absorbed onto the surface of photocatalyst from the solution. Because the amount of TiO_2/D-PVA/MO is determined by step (1) and the experiment conditions (the amount of TiO_2/D-PVA and the intensity of irradiation) are almost constant, it can be concluded that the MO degradation rate is determined by the concentration of MO. The proposed mechanism agrees well with the first-order kinetics result.

$$TiO_2/D\text{-}PVA + MO \underset{k_{-1}}{\overset{k_1}{\rightleftharpoons}} TiO_2/D\text{-}PVA/MO \quad (1)$$

$$TiO_2/D\text{-}PVA/MO + hv \xrightarrow{I_a} TiO_2/D\text{-}PVA^*/MO \quad (2)$$

$$TiO_2/D\text{-}PVA^*/MO \xrightarrow{k_2} TiO_2(e_{cb}^-)/D\text{-}PVA^+/MO \quad (3)$$

$$TiO_2/D\text{-}PVA^+/MO \xrightarrow{k_3} TiO_2/D\text{-}PVA/MO^+ \quad (4)$$

$$e_{cb}^- + O_2 \xrightarrow{k_4} \cdot O_2^- \quad (5)$$

$$\cdot O_2^- + H_2O \xrightarrow{k_5} \cdot OOH + OH^- \quad (6)$$

$$2 \cdot OOH \xrightarrow{k_6} H_2O_2 + O_2 \quad (7)$$

$$\cdot OOH + H_2O + e_{cb}^- \xrightarrow{k_7} H_2O_2 + OH^- \quad (8)$$

$$H_2O_2 + e_{cb}^- \xrightarrow{k_8} \cdot OH + OH^- \quad (9)$$

$$\cdot O_2^- + H_2O_2 \xrightarrow{k_9} \cdot OH + OH^- + O_2 \quad (10)$$

$$\cdot O_2^-/\cdot OH + MO_a/MOa^+ \xrightarrow{k_{10}} \text{Degraded Products} \quad (11)$$

Scheme 2. The mechanism of VL photocatalytic degradation of MO. MO_a and MO_a^+ represent MO and MO^+ absorbed on the surface of TiO_2/D-PVA, respectively.

4. Conclusions

The TiO_2/D-PVA samples were synthesized in one portion of PVA and $Ti(OH)_4$ by means of hydrothermal method. TiO_2/D-PVA exhibited a significant VL photocatalytic activity for the MO degradation in contrast to pure TiO_2 and P25. The VL photocatalytic activity obviously depended on the PVA dosage and hydrothermal temperature. The photocatalyst exhibited the higher activity for MO degradation, prepared at 180 °C with the 1:10 feed ratio of PVA to TiO_2 and hydrothermal reaction time for 6 h. By the hydrothermal process, as $Ti(OH)_4$ was degraded to produce TiO_2, PVA was degraded to produce conjugated unsaturated D-PVA that was doped onto the surface of TiO_2. The VL photocatalytic activity was attributed to the interaction of D-PVA and TiO_2. The rate of VL photodegradation of MO fit with the first-order kinetics.

Acknowledgement

The authors thank for the support of the key project (2006C11172) by Science and Technology Department of Zhejiang Province, China.

References

[1] K.Y. Jung, S.B. Park, Appl. Catal. A 224 (2002) 229–237.
[2] R.M. Mohamed, A.A. Ismail, I. Othman, I.A. Ibrahim, J. Mol. Catal. A: Chem. 238 (2005) 151–157.
[3] M. Gratzel, Nature 414 (2001) 338–344.
[4] M. Gratzel, J. Photochem. Photobiol. C: Photochem. Rev. 4 (2003) 145–153.
[5] J.F. Zhu, F. Chen, J.L. Zhang, H.J. Chen, M. Anpo, J. Photochem. Photobiol. A: Chem. 180 (2006) 196–204.
[6] H. Yamashita, M. Harada, J. Misaka, M. Takeuchi, K. Ikeue, M. Anpo, J. Photochem. Photobiol. A: Chem. 148 (2002) 257–261.
[7] Y. Ishibai, J. Sato, S. Akita, T. Nishikawa, S. Miyagishi, J. Photochem. Photobiol. A: Chem. 188 (2007) 106–111.
[8] J.F. Zhu, Z.G. Deng, F. Chen, J.L. Zhang, H.J. Chen, M. Anpo, J.Z. Huang, L.Z. Zhang, Appl. Catal. B: Environ. 62 (2006) 329–335.
[9] K. Sugiyama, T. Ogawa, N. Saito, Y. Hosoya, T. Yajima, Surf. Coat. Technol. 173–174 (2003) 882–885.
[10] Y.Z. Li, D.S. Hwang, N.H. Lee, S.J. Kim, Chem. Phys. Lett. 404 (2005) 25–29.
[11] D.C. Cronemeyer, Phys. Rev. 113 (1959) 1222–1226.
[12] Y. Suda, H. Kawasaki, T. Ueda, T. Ohshima, Thin Solid Films 475 (2005) 337–341.
[13] S. Yin, Y. Aita, M. Komatsu, T. Sato, J. Eur. Ceram. Soc. 26 (2006) 2735–2742.
[14] S. Mozia, M. Tomaszewska, B. Kosowska, B. Grzmil, Appl. Catal. B: Environ. 55 (2005) 195–200.
[15] C.S. Kuo, Y.H. Tseng, C.H. Huang, Y.Y. Li, J. Mol. Catal. A: Chem. 270 (2007) 93–100.
[16] W.J. Ren, Z.H. Ai, F.L. Jia, L.Z. Zhang, X.X. Fan, Z.G. Zou, Appl. Catal. B: Environ. 69 (2007) 138–144.
[17] C.K. Xu, R. Killmeyer, M.L. Gray, S.U.M. Khan, Appl. Catal. B: Environ. 64 (2006) 312–317.

[18] M. Janus, B. Tryba, M. Inagaki, A.W. Morawaski, Appl. Catal. B: Environ. 52 (2004) 61–67.
[19] M. Inagaki, F. Kojin, B. Tryba, M. Toyoda, Carbon 43 (2005) 1652–1659.
[20] W.K. Hoa, J.C. Yua, S.C. Lee, J. Solid State Chem. 179 (2006) 1171–1176.
[21] D. Chatterjee, A. Mahata, J. Photochem. Photobiol. A: Chem. 153 (2002) 199–204.
[22] D. Chatterjee, A. Mahata, Appl. Catal. B: Environ. 33 (2001) 119–125.
[23] J. Moon, C.Y. Yun, K.W. Chung, M.S. Kang, J. Yi, Catal. Today 87 (2003) 77–86.
[24] B.T. Su, X.H. Liu, X.X. Peng, T. Xiao, Z.X. Su, Mater. Sci. Eng. A 349 (2003) 59–62.
[25] L. Song, R.L. Qiu, Y.Q. Mo, D.D. Zhang, H. Wei, Y. Xiong, Catal. Commun. 8 (2007) 429–433.
[26] P.A. van Hal, M.P.T. Christiaans, M.M. Wienk, J.M. Kroon, R.A.J. Janssen, J. Phys. Chem. B 103 (1999) 4352–4359.
[27] S.V. Chasteen, V. Sholin, S.A. Carter, G. Rumbles, Sol. Energy Mater. Sol. Cells 92 (2008) 651–659.
[28] Y.Q. Gou, D.Y. Chen, Z.X. Su, Appl. Catal. A: Gen. 261 (2004) 15–18.
[29] J.G. Yu, X.J. Zhao, Q.N. Zhao, Thin Solid Films 379 (2000) 7–14.
[30] H. Irie, Y. Watanabe, K. Hashimoto, Chem. Lett. 32 (2003) 772–773.
[31] D.F. Ollis, E. Pelizzetti, Photocatalysis Fundamentals and Applications, John Wiley, New York, 1994.
[32] T. Wu, T. Lin, J. Zhao, H. Hidaka, N. Serpone, Environ. Sci. Technol. 33 (1999) 1379–1387.
[33] Y. Cho, W. Choi, C.H. Lee, T. Hyeon, H.I. Lee, Environ. Sci. Technol. 35 (2001) 966–970.